Comparison of seven compartment models of diffusion in prostate tissue

Sisi Liang[1], Eleftheria Panagiotaki[2], Peng Shi[1], and Roger Bourne[3]

[1]*College of Engineering and Science, Victoria University, Melbourne, Vic, Australia,* [2]*Centre for Medical Image Computing, University College London, London, England, United Kingdom,* [3]*Discipline of Medical Radiation Sciences, Faculty of Health Sciences, University of Sydney, Sydney, NSW, Australia*

Target Audience This work is addressed to biophysical modelers, diffusion MRI researchers, cancer imaging researchers and radiologists.

Purpose One of the aims of clinical diffusion-weighted magnetic resonance imaging (DWI) is the inference of tissue structure properties, particularly pathology, from measurements of diffusion attenuation under conditions of varying diffusion time and diffusion weighting. For this purpose structure-based models are more useful than those that simply provide mathematical descriptions of the signal attenuation profile. For prostate DWI the modeling to date has been largely phenomenological. Recently a three-component structure-based model called VERDICT (Vascular, Extracellular and Restricted Diffusion for Cytometry in Tumors)[1] was utilized to quantify and map histological features of prostate tissue in vivo at 3T. The results suggest VERDICT can discriminate benign and cancerous prostate tissue better than Apparent Diffusion Coefficient[2] and Intravoxel Incoherent Motion[3] models. Motivated by the finding that VERDICT is superior to the two phenomenological models at clinical imaging, this study investigates the non-perfusion components of the VERDICT model in prostate tissue ex vivo at high spatial resolution.

Methods DWI. Two whole prostates were formalin fixed for 48hr. Pulse-gradient spin-echo DWI was performed on a Bruker Biospec 9.4T scanner[4]. Prostate 1: Δ = 20, 40, 80ms, δ = 5ms, b = 105, 279, 589, 1044, 1646, 2403, 3318, 4394, 5631, 7036, 8610, 10354 s/mm^2, 3 orthogonal directions, TE = 28, 48, 88 ms, $SNR_{b=0}$ ~240, FOV 45×45mm, and matrix 32×32; A separate 6-direction diffusion tensor imaging (DTI) acquisition was performed with b = 1599 s/mm^2. Prostate 2: Δ = 10, 20, 40, 60, 80ms, δ = 5ms, b = 50, 147, 275, 430, 607, 806, 1024, 1259, 1512, 1780, 2064, 2362, 2674, 3000 s/mm^2, 3 orthogonal directions, TE = 18, 28, 48, 68, 88 ms, and $SNR_{b=0}$ ~210, FOV 51×42 mm, and matrix 32×25; Separate DTI with b = 1500 s/mm^2. The data was normalized to avoid T_2 dependence.

Diffusion Models. We modeled prostate tissue with 1, 2, or 3 components. For each component, there were four candidate models: 1) a '*Ball*' that assumes Gaussian behavior with no restricting diffusion within cells[5]; 2) a '*Zeppelin*' that describes cylindrically symmetric anisotropic diffusion[5]. 3) a '*Tensor*' which is a full diffusion tensor[6] without symmetry constraints, and 4) a '*Sphere*' describing diffusion inside an impermeable sphere of radius R using the Gaussian phase distribution approximation[7]. Diffusivities were constrained to be within biologically plausible limits so that $0<D<2.3\mu m^2/ms$[8]. For the 'Sphere' model, we constrain the radius to be $0.1<R<20\mu m$. Seven models were fitted to each voxel in four adjacent slices of the two prostates.

Model fitting and ranking. Model fitting was performed in Camino[9]. The models were fitted to the combined DWI and DTI data by nonlinear optimization (employing the Levenberg-Marquardt minimization algorithm in Camino) as in[1]. First we monitored the evolution of the objective function over 1000 runs to assess convergence to the best parameter estimate (lowest objective function) and found that the number of runs required to obtain the best solution in each model with probability > 0.99 was less than 100. Subsequently, for each voxel, we chose the best-fit parameters after 100 perturbations of the starting point to avoid local minima. The Akaike Information Criterion (AIC)[10] was calculated to provide an objective quantitative estimate of the information content of the models. Lower AIC indicates higher model information content, equivalent to less information loss and indicative of superior model prediction performance.

Results Fig. 1A shows the results of model ranking based on AIC. For both prostates, the Zeppelin-sphere was the best model in the majority of voxels. The positional variance diagrams (Fig. 1B) based on AIC ranking illustrate the relative performance of the seven models. For the order of the ranking, there was good agreement between two data sets with some variation of Bi-zeppelin, Ball-zeppelin and Ball-tensor model positions. For Prostate 1 the Bi-ball-zeppelin model did not find a solution within diffusion constraints in the majority of voxels so we ranked it lowest.

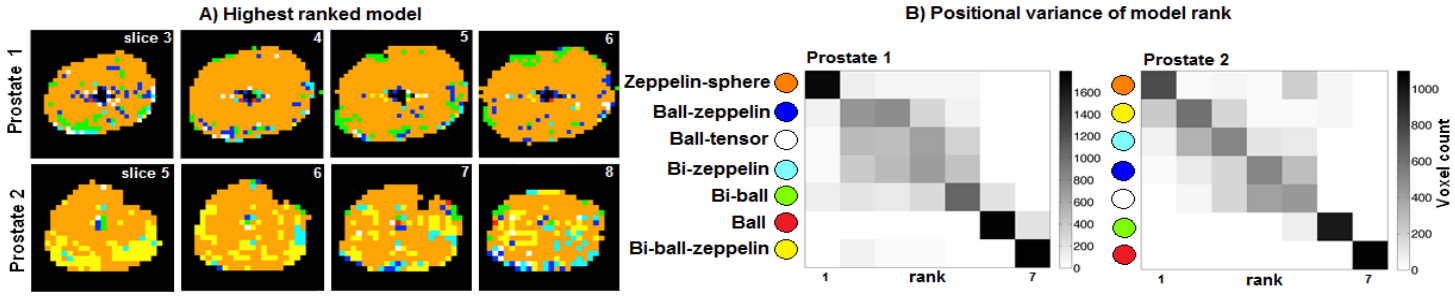

Fig. 1. A) Anatomical distribution of the highest ranked model. B) Variation of model rank position over all intraprostatic voxels.

Discussion & Conclusions The two-component Zeppelin-sphere model consistently ranked higher than other models. All anisotropic two-component models ranked higher than the isotropic two-component 'Bi-ball' model, indicating the presence of significant diffusion anisotropy in the majority of voxels. The Zeppelin-sphere is the only model with a restricted diffusion component – suggesting that explicit modeling of restriction is important in prostate tissue. This finding supports those of the in vivo VERDICT study[1], and specifically characterizes the two true diffusion (non-perfusion) components of that model. It is noteworthy to mention that there are two differences between this study and the in vivo VERDICT study on modeling: first, the VERDICT chose Ball (isotropic) model for the extracellular space and we used Zeppelin (anisotropic) model; second, diffusion coefficients were fixed to certain values in the VERDICT and ours were not.

References

1) Panagiotaki, E, et al. Investigative Radiology 2014 (in press). 2) Eis M, et al. Magn Reson Med 1995 34(6):835-44. 3) Le Bihan D, et al. Radiology 1988 168(2):497-505. 4) Bourne R, et al. Magn Reson Med 2013 70(4):1160-66. 5) Panagiotaki E, et al. NeuroImage 2012 59:2241-54. 6) Basser et al, Biophys J, 1994. 7) Murday and Cotts J Chem Phys 1984. 8) H, W, Z Phys Chem 1982. 9) Cook PA, et al. ISMRM 2006. P2759. 10) Bourne, R, et al., Magn Reson Med 2014 (now published.).